AJNR

Tissue-Specific Imaging Is a Robust Methodology to Differentiate In Vivo T1 Black Holes with Advanced Multiple Sclerosis –Induced Damage

M. Riva, V.N. Ikonomidou, J.J. Ostuni, P. van Gelderen, S. Auh, J.M. Ohayon, F. Tovar-Moll, N.D. Richert, J.H. Duyn and F. Bagnato

AJNR Am J Neuroradiol 2009, 30 (7) 1394-1401
doi: https://doi.org/10.3174/ajnr.A1573
http://www.ajnr.org/content/30/7/1394

ORIGINAL RESEARCH

Tissue-Specific Imaging Is a Robust Methodology to Differentiate In Vivo T1 Black Holes with Advanced Multiple Sclerosis–Induced Damage

M. Riva
V.N. Ikonomidou
J.J. Ostuni
P. van Gelderen
S. Auh
J.M. Ohayon
F. Tovar-Moll
N.D. Richert
J.H. Duyn
F. Bagnato

BACKGROUND AND PURPOSE: Brains of patients with multiple sclerosis (MS) characteristically have "black holes" (BHs), hypointense lesions on T1-weighted (T1W) spin-echo (SE) images. Although conventional MR imaging can disclose chronic BHs (CBHs), it cannot stage the degree of their pathologic condition. Tissue-specific imaging (TSI), a recently introduced MR imaging technique, allows selective visualization of white matter (WM), gray matter (GM), and CSF on the basis of T1 values of classes of tissue. We investigated the ability of TSI-CSF to separate CBHs with longer T1 values, which likely represent lesions containing higher levels of destruction and unbound water.

MATERIALS AND METHODS: Eighteen patients with MS, who had already undergone MR imaging twice (24 months apart) on a 1.5T scanner, underwent a 3T MR imaging examination. Images acquired at 1.5T included sequences of precontrast and postcontrast T1W SE, T2-weighted (T2W) SE, and magnetization transfer (MT). Sequences obtained at 3T included precontrast and postcontrast T1W SE, T2W SE, T1 inversion recovery prepared fast spoiled gradient recalled-echo (IR-FSPGR) and TSI. A BH on the 3T-IR-FSPGR was defined as a CBH if seen as a hypointense, nonenhancing lesion with a corresponding T2 abnormality for at least 24 months. CBHs were separated into 2 groups: those visible as hyperintensities on TSI-CSF (group A), and those not appearing on the TSI-CSF (group B).

RESULTS: Mean MT ratios of group-A lesions (0.22 ± 0.06, 0.13–0.35) were lower ($F_{1,13} = 60.39$; $P <$ .0001) than those of group-B lesions (0.32 ± 0.03, 0.27–0.36).

CONCLUSIONS: Group-A lesions had more advanced tissue damage; thus, TSI is a potentially valuable method for qualitative and objective identification.

Patients with multiple sclerosis (MS) are typically injected with a complex of the contrast agent gadolinium (Gd) during the MR imaging regimen to identify areas of inflammatory activity in brain and spinal cord tissue. These areas, termed *contrast-enhancing lesions* (CELs), are seen as hyperintense lesions on T1-weighted (T1W) MR imaging.[1] The MR imaging lifespan of CELs varies from weeks[2] to a few months,[3,4] most CELs resolving within 2 months.[3,4] Up to 80% of these hyperintense CELs are seen as hypointense lesions on T1-weighted spin-echo (T1W SE) images obtained before injection of the contrast agent.[5] Those hypointensities, known as black holes (BHs),[6] are thought to correspond to areas where transient edema accompanying inflammation accumulates and are referred to as acute BHs (ABHs). Most of the ABHs disappear when the enhancement ceases. Only a portion (ie, 25%–40%) persist as chronic BHs (CBHs).[7-11] Although some of the CBHs shrink as time progresses,[12] the overall MR imaging characteristics of most CBHs change little, even 12 months after resolution of the enhancement[12]; that is to say, almost no CBHs disappear after the 24-month period following the loss of enhancement.[11]

Because CBH load accounts for approximately 50% of the variance of physical disability in patients with MS[5,13,14] and is one of the strongest identifiable predictors of cerebral atrophy,[15] it is considered an important imaging metric of disease progression.[16] Motivated by this finding and in an attempt to understand its biologic basis, researchers have performed numerous postmortem combined MR imaging and pathologic studies[17-19] to identify the pathologic correlates of CBHs. These studies showed that CBHs are likely not a biologic unique identity because a fair amount of heterogeneity in the degrees of demyelination,[20,21] matrix destruction, increase in extracellular fluid,[22] and reduced axonal attenuation[7] may be present. Such heterogeneity was indicated on MR imaging by differences in magnetization transfer ratios (MTRs).[17] Different rates of decreased MTRs are associated with different levels of destructive pathologic changes. Specifically, low MTR values,[7] close to those of the CSF, are seen in some BHs and likely indicate that accumulation of freely moving extracellular fluid in part characterizes the final stage of BHs in MS.[23]

Conventional T1W SE imaging allows the identification of CBHs but has 2 important limitations. First, by simply looking at T1W SE images for the presence or absence of BHs and without performing any quantitative measurements such as signal intensity computation or quantitative T1, the observer is unable to rate the degree of tissue destruction that is known to exist. Second, it is well known that the appearance of CBHs on MR imaging may vary, depending on several MR imaging–related technical parameters such as TR and TE, or strength of the magnetic field used. These factors make the measurement

Received November 7, 2008; accepted after revision January 31, 2009.

From the Neuroimmunology Branch (M.R., V.N.I., J.J.O., J.M.O., F.T-.M., N.D.R., F.B.); Advanced MRI Section, LFMI (V.N.I., P.v.G., J.H.D.); and Office of the Clinical Director (S.A.), NINDS, National Institutes of Health, Bethesda, Md.

This work was supported by the Intramural Research Program of the NINDS, NIH. Dr. F. Tovar-Moll was supported also by the LABS–D'Or Hospital Network, Rio de Janeiro, Brazil.

Previously presented at: Annual Meeting of the American Academy of Neurology, San Diego, Calif; April 5, 2006.

Please address correspondence to Francesca Bagnato, MD, PhD, Neuroimmunology Branch, NINDS, NIH, Building 10, Room 5C103, 10 Center Dr, Bethesda, MD 20892-1400; e-mail: bagnatof@ninds.nih.gov

DOI 10.3174/ajnr.A1573

Demographic, clinical, and MR imaging characteristics of patients at the time of 3T MR imaging

	Patients with RRMS ($n = 9$)	Patients with SPMS ($n = 7$)	P value*
Age (y)	41.3 ± 6.3 (range, 32–53)	50.2 ± 6.0 (range, 41–56)	.012
Sex	5 women, 4 men	6 women, 1 man	NS
Years since MS onset	10.4 ± 6.2 (range, 3–20)	18.4 ± 5.2 (range, 13–28)	.016
EDSS	1.9 ± 1.1 (range, 0–4)	6.0 ± 0.6 (range, 5–6.5)	<.0001
PASAT	48.7 ± 12.8 (range, 22–60)	31.2 ± 8.1 (range, 21–45)	.008
BPF	0.81 ± 0.05 (range, 0.76–0.92)	0.75 ± 0.04 (range, 0.71–0.81)	.014
T2-LV (cm^3)	11.5 ± 8.8 (range, 0.78–25.5)	12.6 ± 8.4 (range, 4.6–30.1)	NS
Number of patients with CELs	1†	0	N/A
CBHs (number)	48.9 ± 51.5 (range, 0–126)	37.4 ± 19.7 (range, 19–76)	NS
CBHs (volume in cm^3)	2.8 ± 3.3 (range, 0.1–9.6)	3.2 ± 2.7 (range, 0.8–8.4)	NS
CBHs-LV/T2-LV (%)	16.9 ± 11.7 (range, 3–34)	24.1 ± 10.3 (range, 14–48)	NS
Undergoing therapies			
Interferon beta	3	3	
Daclizumab	4	–	
Other treatments	–	2	
None	2	2	

Note:—RRMS indicates relapsing-remitting multiple sclerosis; SPMS, secondary-progressive multiple sclerosis; EDSS, Expanded Disability Status Scale; PASAT, Paced Auditory Serial Addition Test; BPF, brain parenchyma fraction; T2-LV, T2 lesion volume; CELs, contrast-enhancing lesions; CBHs, chronic black holes; N/A, not applicable; NS, not significant.
* P values are significant if $P \leq .05$.
† A single patient had 1 CEL in the corpus callosum (see text in the Results section).

of CBHs still partially subjective and weaken its potential to become a useful tool for multicenter clinical trials.

To overcome these limitations, in our study we set out to assess the ability of an MR imaging technique developed at the National Institutes of Health (NIH), namely Tissue-Specific Imaging (TSI),[24] to selectively visualize CBHs in patients with MS and severe disease pathologic changes. Specifically, we hypothesized that 1) only part of the MS CBHs are visible on a TSI-CSF image; and 2) CBHs visible on TSI-CSF represent areas with more advanced disease pathologic changes dominated by severely unstructured tissue and unbound molecules, which confer long T1 values to tissues in general[25] and lesions. To test this hypothesis, we computed and compared the MTRs of CBHs appearing as visible lesions in the TSI-CSF and those not corresponding to abnormal signal intensity on TSI-CSF. We expected MTR values of TSI-CSF-CBHs to be significantly lower and closer to the CSF-MTRs than those of CBHs not visible on TSI-CSF.

Materials and Methods

Patients and Study Design

We performed our study at the NIH in Bethesda, Md. The Institutional Research Board of the National Institute of Neurologic Disorders and Stroke approved the study. We obtained informed written consent from all subjects.

Eighteen patients with clinically definite MS,[26] free from corticosteroids and clinical relapses for at least 3 months, entered into the study. All patients were required to have had two 1.5T MR imaging examinations, 24 months apart, obtained by the Neuroimmunology Branch as part of the regular clinical follow-up, and to be willing to participate in a 3T MR imaging study no later than 1 month from the last 1.5T scan (60 days only in the case of 1 patient). In every case, all 3 scans were obtained at least 3 months after a clinical relapse or steroid administration. All patients underwent a clinical examination on the same day as each MR imaging study. We rated physical disability using the Expanded Disability Status Scale (EDSS)[27] and the Paced Auditory Serial Addition Test (PASAT)[28] scores. Demographic, clinical, and MR imaging characteristics of patients at the time of the 3T MR imaging study are reported in the accompanying Table.

Image Acquisition

1.5T MR imaging. We performed both 1.5T examinations using an 8-channel high resolution head coil (Invivo Corp., Gainesville, Fla). Forty-two contiguous 3-mm sections were obtained axially by use of a 24-cm FOV and a matrix size of 256 × 192. Images were acquired in the following order: 1) fast SE (FSE) T2-weighted (T2W) image with TR 3400 ms, TE 105 ms; 2) T1W magnetization transfer imaging (MTI) with TR 600 ms and TE 16 ms, with and without (for the 1.5T examination performed at the time of the 3T MR imaging) an MT pulse of 600 Hz below water frequency[29]; and 3) contrast-enhanced T1W SE image 10 minutes after intravenous injection of 0.1 mmol/kg of Gd-DTPA (Magnevist; Bayer HealthCare, Wayne, NJ). At the Neuroimmunology Branch, MTI is part of the routine MR imaging offered to each patient.

3T MR imaging. At 3T, we acquired scans using an 8-channel high resolution head coil (Invivo Corp.). On the axial plane, a T1 inversion recovery prepared fast-spoiled gradient recalled-echo (IR-FSPGR) image and a TSI were acquired. We obtained the IR-FSPGR using a 1.0-mm section thickness; 24-cm FOV; matrix size, 256 × 256; TE, 3 ms; TR, 7.5 ms; bandwidth, 31.25 kHz; FA, 16°, and acquisition time, 7:31 minutes.

The TSI was implemented as previously described.[24] In an overall per slice TR of 6 s, 3 echo-planar image (EPI) acquisition trains were implemented at times 0 ms, 3675 ms, and 5821 ms, with flip angles (FA) for the imaging pulses 83°, 17°, and 62°, respectively. Two adiabatic inversion pulses were used at 3195 ms and 5383 ms. Sensitivity encoding rate 2 acceleration was used to achieve whole brain coverage with matrix size 144 × 112 × 110 with 1.5-mm^3 isotropic resolution in 11 minutes. TE was set to 35 ms. Navigator echo correction was used to minimize phase errors between subsequent excitations. The resulting raw images were combined assuming average T1 values of 800 ms, 1550 ms, and 4000 ms for white matter (WM), gray matter (GM), and CSF, respectively. Finally, conventional precontrast and postcontrast T1W SE and T2W FSE images were obtained. Conventional images at 3T were analyzed only to ascertain of the presence of

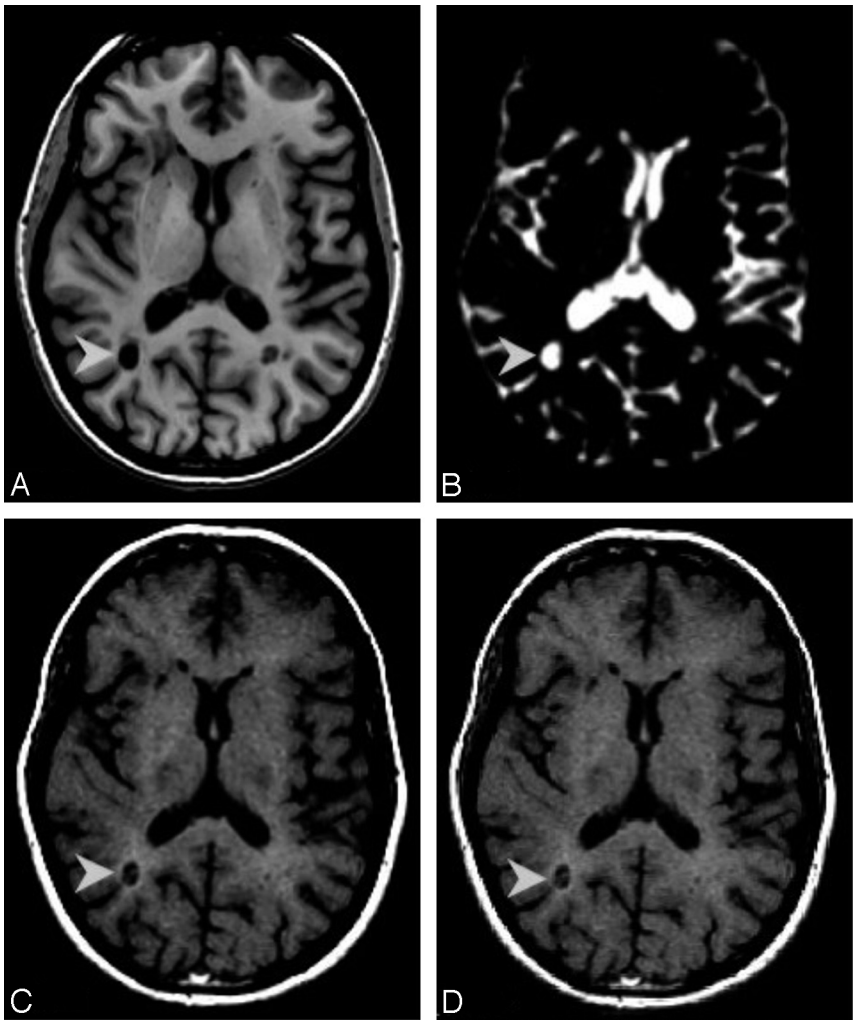

Fig 1. *A,* Axial view of IR-FSPGR image. *B,* Axial view of 3D-TSI-CSF image. *C,* Axial view of T1-weighted image acquired at the time of the 3T MR imaging. *D,* Axial view of T1-weighted image acquired 24 months before images reported in *A–C*. *A–D* shows a group-A lesion (*arrowheads*). Only one of the lesions identified on MR imaging is discussed as an example. It can be seen that the BH in *A* corresponds to a hyperintense area on the relative TSI volume (*B*). The BH marked here is defined as CBH because it was present 24 months before the 3T study (*D*).

active lesions and to compute the T2 lesion volume. We obtained 54 interleaved contiguous 2.4-mm sections axially using a 24-cm FOV and a matrix size of 256 × 256. Images were acquired in the following order: 1) FSE T2W image with TR 5100 ms and TE 120 ms; 2) T1W precontrast and postcontrast image obtained 10 minutes after intravenous injection of 0.1 mmol/kg of Gd-DTPA (Magnevist) with TR 700 ms and TE 11 ms.

Image Analysis

Definition and identification of CBHs. CBHs were identified as follows: first, all hypointensities on IR-FSPGR were identified. These hypointensities were defined as CBHs if they met the following requirements: 1) they had a corresponding hypointense lesion on both the T1W SE image obtained with the 1.5T magnet, which, in turn, corresponded to a hyperintense lesion on the T2W-SE image; and 2) they did not correspond to CEL on the T1W SE images at both 1.5T MR images and the 3T scan. Once those CBHs were identified, they were separated in 2 groups, namely group A and group B. Group-A CBHs corresponded to hyperintense lesions on the TSI-CSF image. Group-B CBHs were CBHs that did not appear as hyperintensities on the 3D-TSI-CSF image. Figures 1 and 2 show examples of group-A and group-B lesions, respectively. Lastly, MTRs of group-A and group-B lesions were computed.

The brain parenchyma fraction (BPF) from the IR-FSPGR and the T2 lesion volume (T2-LV) from the T2W image acquired with the 3T scanner were also calculated.

In the following paragraphs, methodologies used for image analysis are described in detail.

Postprocessing Analysis

Image registration. The 1.5T magnetization transfer-saturation pulse on (MT-ON) and magnetization transfer-saturation pulse off (MT-OFF) (ie, T1W SE) images acquired at the time of the 3T MR imaging, the T1W SE image obtained 24 months before, as well as the TSI-CSF images were resectioned and registered to the IR-FSPGR with use of an affine registration as implemented in the Functional Linear Image Registration Tool 3.1 (FLIRT; Functional Magnetic Resonance Imaging of the Brain Centre, University of Oxford, UK, http://www.fmrib.ox.ac.uk). The Brain Extraction Tool, version 1.2, available in the FMRIB library, was used to remove extrameningeal tissue from whole-head volumes. A low-pass filtering algorithm[30] was ap-

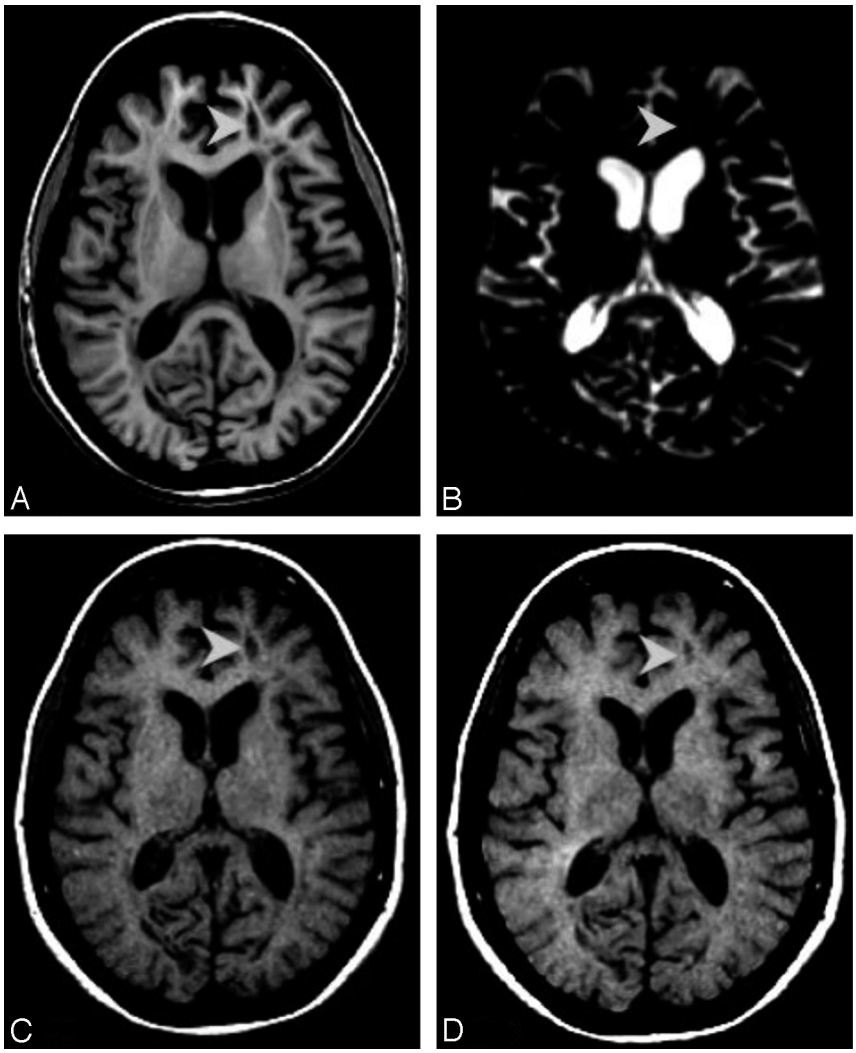

Fig 2. *A*, Axial view of IR-FSPGR image. *B*, Axial view of 3D-TSI-CSF image. *C*, Axial view of T1-weighted image acquired at the time of the 3T MR imaging. *D*, Axial view of T1-weighted image acquired 24 months before images reported in *A–C*. *A–D* reports a group-B lesion (*arrowheads*). Compared with group A, group-B chronic BHs do not have a corresponding hyperintense area on the 3D-TSI-CSF image (*B*), thought to be present as an area of hypointensity on IR-FSPGR and T1-weighted images (*A,C*).

plied to the entire dataset of brain IR-FSPGRs to compensate for the nonuniformity of the magnetic field.

Group-A and Group-B lesions identification. An observer (M.R.) blinded to the clinical features of the patients, marked the hypointense lesions on the IR-FSPGR image according to the strategy previously described.[31] Lesions were marked on the IR-FSPGR image to ensure that the identification was obtained on the image with the highest resolution. Quality of the lesion masks was confirmed by a second observer (F.B.). Because of the shimming-related signal intensity loss in EPI sequences near the cranial air cavities, only lesions above the mammillary bodies were included in the study analysis. Hypointensities identified and selected on the IR-FSPGR image were first overlaid on both 1.5T T1W MT-OFF images. Lesions were resized according to their extent on both 1.5T studies. The resulting group of regions of interest (ROIs) was overlaid on the 3D-TSI-CSF image. Group-A and group-B lesions were identified on the basis of their appearance on this image sequence by consensus of 3 investigators (M.R., F.B., and V.N.I.). To ensure an objective identification of lesions and avoid inclusion as lesions signal intensity changes from artifacts, we adopted 2 different criteria for group-A or TSI-CSF lesions classification. The first lesion category included regions where signal intensity changed equal or greater than 5 SDs more than the signal intensity of the contralateral suppressed normal-appearing WM (NAWM). In the second set of criteria, no lesion-intensity threshold was used. All of the analyses subsequently obtained were performed twice on the basis of the 2 different criteria of classification. We then computed the number and volume of each group of ROIs with both criteria using IDL (ITT Visual Information Solutions, Boulder, Colo).

Computation of group-A and group-B lesions, normal-appearing GM and WM ROI-MTR. We performed MT analysis using MEDx 3.43 (Medical Numerics, Germantown, Md),[3,29] and we calculated MTR maps for each patient by using a method previously described.[32] To avoid biases because of partial-volume effect in the MTR measurements,[29] we did not include ROIs containing 10 or less voxels in the lesion burden and MTR computations.

For each patient, group-A and group-B ROIs were overlaid on the MTR image with precise reference to CBH marked on T1W and 3D-TSI-CSF volumes, previously registered to MT-OFF and MT-ON. Six 4×4 ROIs in NAWM, normal-appearing GM (NAGM) of the basal ganglia (BG), and CSF were also positioned. The latter was done to provide MTR reference values of our images. MTR measurements

were performed on the 1.5T MR imaging study acquired no more than a month before the 3T scan.

A 0.01% unit threshold was used to minimize CSF partial-volume effects. Mean MTRs for both groups of lesions, A and B, were obtained. Because of image artifacts, MTR values were not computed for the image of 1 patient.

BPF computation. BPFs were measured on the 3T IR-FSPGR image with the Structural Imaging Evaluation of Normalized Atrophy (SIENAx) software.[33]

T2-LV computation. Before marking hyperintense lesions, care was taken to ensure that the observer (A.C.) reached a coefficient of variation in lesions computation less than 5% with respect to 2 independent investigators (F.T.-M. and F.B.). This observer, blinded to the clinical features of the patients, then marked the hyperintense lesions on the T2W SE images according to the strategy previously described.[31]

The T2 lesion masks were generated by use of MEDx,[34] and they were all checked by a second, more experienced radiologist (F.T.-M.). LV was computed with use of IDL (ITT Visual Information Solutions), after thresholding to a constant intensity level. For the purpose of this study and to be consistent with CBH measurements, we excluded lesions identified below the mammillary bodies.

Statistical Analyses

Intraclass correlation coefficient (ICC) analysis was used to analyze correlation in lesion number and volume between the lesions computed with and without the intensity lesions-threshold. Two-sample *t* tests for continuous variables and χ^2 tests for categoric variables were performed to compare 2 independent groups of patients (ie, patients with relapsing-remitting MS [RRMS] and secondary-progressive MS [SPMS]), only for the variables regarding demographic, clinical, and MR imaging characteristics presented in the Table.

For each subject, the total number of lesions in groups A and B were calculated. In addition, for each subject, volumes and MTRs were averaged separately for lesions of group A and group B. These summary measurements per subject were treated as 2 correlated observations within the same patient. A generalized linear mixed-effects model was used to compare the total number of lesions between groups A and B, assuming that it followed a negative binomial distribution, accounting for the overdispersion of a Poisson variable, regardless of disease stage. In a similar fashion, a linear mixed-effects model assuming compound symmetry covariance structure was used to compare either volume or MTR, respectively, between groups A and B.

A generalized linear model for the total number of lesions and 2-sampled *t* tests for each of volume, MTR, and volume ratio delineated the difference between patients with RRMS and those with SPMS, in groups A and B.

We examined the differences in MTR values among 5 different brain components' group-A and group-B lesions, and ROIs placed in CSF, NAWM, and BG, by using a linear mixed-effects model. The model assumed compound symmetry covariance structure, followed by Bonferroni-corrected post hoc multiple pair-wise comparisons of interest, NAWM/BG, BG/group B, group B/A, group A/CSF, NAWM/ group B, and BG/group A.

Correlation analyses exploring the association between group-A and group-B lesion number, volume, mean MTR, and ratio to CBHs with clinical scales of disability (ie, EDSS, PASAT), years of disease, and other MR imaging parameters were performed with the Spearman rank correlation coefficient.

Data were reported as mean ± SD and range, unless otherwise indicated. All analyses were conducted with the use of SPSS (version 14.0; SPSS, Chicago, Ill) and SAS (version 9.1.3; SAS Institute, Cary, NC) software. Bonferroni correction for multiple comparisons was used if necessary, as explained throughout the study. *P* values of less than .05 were considered as statistically significant, unless otherwise specified.

Results

Two levels of analyses are herein presented. First, differences in MTRs, number, and volume between group-A and group-B lesions are described. Second, correlations between group-A and group-B lesion number, volume, MTR, and other clinical or MR imaging metrics of the disease are presented. As explained in the Methods section, both types of analyses were run twice. In the first course of analyses, group-A and group-B lesions were segregated on the basis of threshold intensity on TSI-CSF. In the second course, lesions were classified as group-A and group-B only on the basis of visual inspection. The estimated value of the ICC between the 2 methods was 0.986 for lesion number and 0.989 for lesion volume, indicating excellent reliability. Given the ICC values and because no differences were seen in the outcome of the analyses when the different criteria of categorization were used, we report, for clarity only, the outcome of the results obtained when categorizing lesions by using the threshold intensity.

Incidence, Characterization, and Clinical Significance of Group-A and Group-B CBHs

MR imaging evaluation of 1 patient was not feasible because of image artifacts. Also, T2-LV was not computed in 1 patient because no T2W images from the 3T scanner were available for this person. Therefore, all the data analysis done and presented here excludes these 2 patients and includes 16 of the original cohort of 18.

Comparisons in number, volume, and mean MTR of group-A and group-B lesions. No signal intensity abnormalities or TSI-CSF lesions were identified other than those corresponding to a CBH. None of the patients was found to have CEL at the 3T MR imaging except for 1 patient who had a small CEL on the corpus callosum not corresponding to any identified CBH.

The mean number of group-A lesions (14.69 ± 14.24; range, 0–45) was significantly smaller ($F_{1,14} = 46.29$; $P < .0001$) than the number of group-B lesions (31.13 ± 26.03; range, 3–84). Although not significantly, the mean volume of group-A lesions was larger (1.95 ± 2.20; range, 0.01–6.54 cm^3) than the volume of group-B lesions (1.21 ± 1.03; range, 0.074–3.43 cm^3; $F_{1,13} = 2.23$; $P = .16$).

Mean MTR values of group-A lesions (0.22 ± 0.06; range, 0.13–0.35) were significantly lower ($F_{1,13} = 60.39$; $P < .0001$) than mean MTRs of group-B lesions (0.32 ± 0.03; range, 0.27–0.36). *P* values presented in this session were significant if less than or equal to .05/3, (ie, ≤ .017 on Bonferroni correction).

Comparisons of MTR values among ROIs of different regions of the brain and group-A and group-B lesions. Figure 3 shows the mean MTRs of ROIs placed in NAWM, BG, CSF, and mean MTR values of group-A and group-B lesions. There was a highly significant difference ($F_{4,56} = 525.31$; $P <$

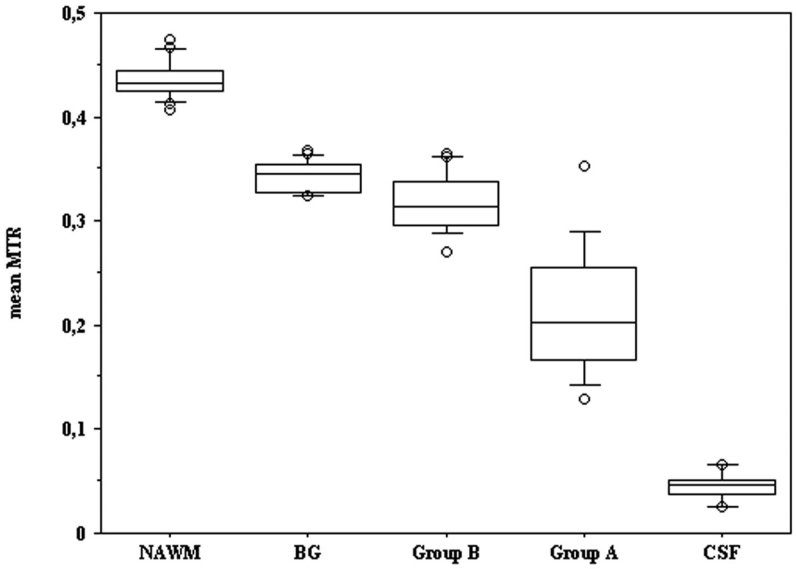

Fig 3. The figure represents the box plot distribution of mean MTR values of NAWM, the BG, group-B lesions, group-A lesions, and CSF. Although group-B and group-A lesions show a wider distribution, it is possible to note a separation among all observed groups.

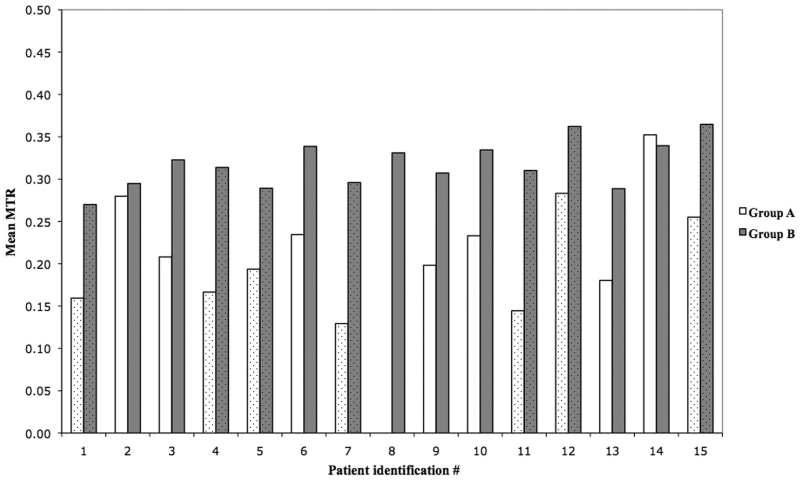

Fig 4. The white bars represent group-A lesions; the gray bars represent group-B lesions. Patients with SPMS are marked with dotted columns. The graph reports the distribution of the mean MTR of group-A and group-B lesions per patient. The data refer to 15 patients. Of the 18 examined, 1 was excluded from the MTR evaluation because of the poor image quality and 1 because of presenting with no T2W image. Of the remaining 16 patients, all except 1 patient had at least 1 CBH.

.0001) among the MTR of the different brain components. Post hoc multiple pair-wise comparisons for the following pairs NAWM/BG, NAWM/group B, BG/group B, BG/group A, group B/A, group A/CSF showed a significant (Bonferroni corrected $P < .0001$) difference in each of the pairs analyzed except for BG/group B.

Occurrence of Group-A and Group-B Lesions in Patients with RRMS and SPMS and Correlations between Clinical and MR Imaging Metrics in Patients with RRMS and SPMS

All patients except 1 had at least 1 CBH; group-A lesions were present in all of the patients with CBHs but 1 (ie, patient 8 in Fig 4). This patient had RRMS. Disease duration was 9 years, and EDSS score was 1.5.

For the remaining patients, as one can see from Fig 4, MTR values of group-A lesions were consistently lower than those of group-B lesions except for 1 patient, who also exhibited peculiarly small volumes of group-A lesions.

There were no significant differences in number, volume, and MTR of group-A or group-B lesions between patients with RRMS and those with SPMS. Although not significant, the ratio of group-A lesion volume (ie, group-A volume/CBHs volume) was larger ($t_{12} = -1.95$; $P = .0744$) in subjects with SPMS compared with subjects with RRMS.

The correlations between group-A and group-B lesion number, volume, MTR, disease duration, EDSS, PASAT, BPF, and T2-LV were also examined. No significant correlations between clinical scales and group-A and group-B lesion number, volume, and MTR emerged, though patients with a higher ratio (in volume) of group-A lesions tended to have longer disease duration ($r = 0.547$; $P = .043$).

Barely significant correlations were seen between the ratio

of the volumes of group-A lesion/CBHs and BPF ($r = -0.534$; $P = .049$) or T2-LV ($r = 0.556$; $P = .039$).

Discussion

TSI includes 2 inversion pulses and 3 3D-EPI acquisitions with different T1 weighting. The latter are combined to produce 3 images that selectively show WM, GM, or CSF only. Thus, in each TSI image, 2 tissue types are suppressed on the basis of their average T1 values, in a manner similar to double inversion recovery (DIR).[35] Although the TSI-GM image is very similar to the DIR images,[36-38] TSI adds the advantage of the other 2 images. In this study, we focus on the TSI-CSF-image, which, in a previous work on healthy brains,[24] was shown to selectively depict only components with long T1 values. These correspond to areas where a substantial amount of liquid and unbound freely moving water are present[25] and are matched with CSF in previous reported work.[24]

The results presented in this study show that TSI-CSF allows the differentiation both qualitatively and objectively of a subset of CBHs in which more advanced MS-induced damage is probably present. Two levels of results are herein discussed and interpreted. First, we focus on differences in MTR values between the 2 groups of lesions and the possible biologic correlates of our MTR findings on the basis of previous reports. Second, we direct our focus to the clinical significance of our results. Limitations of our study and future plans of the group to overcome those limitations are proposed at the end.

TSI-CSF CBHs Exhibit Significantly Lower MTR Values Compared with CBHs not Appearing on TSI-CSF

In accordance with our working hypothesis, the MTRs of group-A CBHs (TSI-CSF lesions) were lower than those of group-B CBHs and also closer to CSF MTRs. The latter is a captivating finding. It shows for, the first time in vivo, that even by classifying CBHs on the basis of a relatively long duration in time, during which lesions were shown to be relatively stable in their appearance,[11] high heterogeneity exists in their underlying pathologic substrate.

Although the mean number and volume of CBHs were quite heterogeneous across patients, mean MTR values were similar, likely reflecting interpatient and intrapatient consistency of the pathologic substrate classified by each lesion group. Specifically, if one excludes patient 14, whose MTR values of group-A lesions were likely biased by partial-volume artifacts, presumably resulting from the small volume of this group of CBHs, it can be seen that patient MTR values of group-B lesions were always higher than the highest observed MTRs of group-A lesions.

The mean MTRs of group-A lesions reported here (eg, 0.22) corresponds to a range of axonal density of 40% to 50% described by previous authors in postmortem studies. Conversely, the mean MTR value of group-B lesions is compatible with a higher degree (eg, up to 90%) of axonal density.[39] We recognize that care needs to be taken when comparing our results with previously reported pathologic findings. It has been proven that antemortem and postmortem MTRs are similar if the same sequence is used.[40] The latter implies that potential small biases resulting from differences in magnet and MT sequences between our in vivo findings and previous postmortem reports from other authors need to be considered. In a cumulative fashion, however, we believe that, at the present time, we can conclude that group-A lesions correspond to areas of severe demyelination, which, in turn, correlate with lower axon numbers.[40]

Correlations between Imaging and Clinical Data

Once TSI-CSF CBHs were identified and characterized, we investigated whether those lesions were associated with clinical or other MR imaging measures reflecting advanced disease.

No correlations of statistical relevance were found between TSI-CSF lesion volume, number, and MTR and clinical scales of disability, EDSS, and PASAT. Several explanations may be proposed to enlighten this finding. First, statistically significant differences might have been masked by the limited number of patients enrolled. The primary aim of this exploratory study was to validate the use of TSI-CSF for the identification of MS lesions. Therefore, we did not perform sample size calculations a priori to allow correlation between MR imaging and clinical findings

Had this been done, we could have unambiguously answered whether TSI-CSF lesions are a powerful metric of physical and cognitive disability. In addition, because we computed the volume and the number of only those lesions lying above the mammillary bodies to avoid potential off-resonance–related problems in TSI, our load computation could be an underestimate of the actual value. In light of the impact that lesions located in the posterior fossa or in the brain stem have on the EDSS score,[41] we acknowledge that the used reference level could have weakened the correlations analysis performed.

Is not surprising that a trend was observed showing patients with SPMS as having a greater volume percentage of group-A lesions than patients with RRMS. Also, greater volume percentage of group-A lesions was found in patients with longer disease duration. The findings support the notion that a greater lesion burden composed of highly destructive CBH affects patients in an advanced stage of the disease. In addition, T2-LV as well as BPF correlated significantly with the absolute or relative load of group-A lesions. Again, being both T2 lesions and brain atrophy reflections of more advanced disease occurring in MS,[42,43] our result supports the evidence that occurrence of group-A CBHs is a sign of a global, more destructive course of MS.

Limitations of the Study

Possible limitations of our study need to be addressed before we draw our conclusions. First, as discussed above, the small sample size precluded any definitive conclusion regarding the clinical significance of our findings. Second, the precise characterization of the pathologic features of the lesions went beyond the achievability of our study because postmortem data were missing.

In vivo and postmortem work is ongoing in our group to better characterize the specificity of CSF lesions. Although no other lesions except those corresponding to CBHs were identified in our images, it remains unknown whether other types of lesions, particularly CELs, may still transiently be visible on TSI-CSF. The latter is an interesting work in progress in our

group and will yield greater insight about the specificity of TSI-CSF MR imaging.

Conclusions

Despite these limitations, we believe our work is a strong example of the originality and relevance of the TSI-CSF image for patients with MS. Our study proposes a methodology for the objective differentiation of in vivo CBHs with more advanced MS-induced neurodegenerative damage. The power of the novel definition of CBHs provided by TSI could be useful to 1) identify more advanced lesions during the course of MS or any other brain-related neurodegenerative disease, and 2) measure potential neuroprotective effects of experimental drugs in clinical trials.

Acknowledgments

We thank all of the patients and their families for their time, patience, and cooperation. We also thank Roger Stone from the NIB-NINDS and Devera Schoenberg, from the Clinical Director Office of the NINDS for editing the material and for data base maintenance, Mary Ehrmantraut, CRNP, for clinical assistance and critical editing of the manuscript, Kadeem Richardson and Annie W Chiu for assistance in postprocessing, and Dr. Henry McFarland for all of his important insights at every step of the project.

References

1. Grossman RI, Gonzalez-Scarano F, Atlas SW, et al. **Multiple sclerosis: gadolinium enhancement in MR imaging.** *Radiology* 1986;161:721–25
2. Cotton F, Weiner HL, Jolesz FA, et al. **MRI contrast uptake in new lesions in relapsing-remitting MS followed at weekly intervals.** *Neurology* 2003;60:640–46
3. Gupta S, Solomon JM, Tasciyan TA, et al. **Interferon-beta-1b effects on reenhancing lesions in patients with multiple sclerosis.** *Mult Scler* 2005;11:658–68
4. Harris JO, Frank JA, Patronas N, et al. **Serial gadolinium-enhanced magnetic resonance imaging scans in patients with early, relapsing-remitting multiple sclerosis: implications for clinical trials and natural history.** *Ann Neurol* 1991;29:548–55
5. Van Walderveen MA, Lycklama A, Nijeholt GJ, et al. **Hypointense lesions on T1-weighted spin-echo magnetic resonance imaging: relation to clinical characteristics in subgroups of patients with multiple sclerosis.** *Arch Neurol* 2001;58:76–81
6. Bagnato F, Evangelou I, Gaindh D, et al. **The role of interferon beta in T1-hypointese black holes in multiple sclerosis.** *Expert Opin Biol Ther* 2007;7:1079–91
7. van Waesberghe JH, Kamphorst W, De Groot CJ, et al. **Axonal loss in multiple sclerosis lesions: magnetic resonance imaging insights into substrates of disability.** *Ann Neurol* 1999;46:747–54
8. Ciccarelli O, Giugni E, Paolillo A, et al. **Magnetic resonance outcome of new enhancing lesions in patients with relapsing-remitting multiple sclerosis.** *Eur J Neurol* 1999;6:455–59
9. Filippi M, Rovaris M, Rocca MA, et al. **Glatimerar acetate reduces the proportion of new MS lesions evolving into "black holes".** *Neurology* 2001;57:731–33
10. Brex PA, Molyneux PD, Smiddy P, et al. **The effect of IFNbeta-1b on the evolution of enhancing lesions in secondary progressive MS.** *Neurology* 2001;57:2185–90
11. Bagnato F, Jeffries N, Richert N, et al. **Evolution of T1 black holes in patients with multiple sclerosis imaged monthly for 4 years.** *Brain* 2003;126:1782–89
12. Freitag P, Mueller B, Radue EW, et al. **Individual changes of chronic black holes.** *Mult Scler* 2001;7 S1, P094
13. Truyen L, van Waesberghe JH, van Walderveen MA, et al. **Accumulation of hypointense lesions ("black holes") on T1 spin-echo MRI correlates with disease progression in multiple sclerosis.** *Neurology* 1996;47:1469–76
14. Barkhof F, van Waesberghe JH, Filippi M, et al. **European Study Group on Interferon beta-1b in Secondary Progressive Multiple Sclerosis. T1 hypointense lesions in secondary progressive multiple sclerosis: effect of interferon beta-1b treatment**. *Brain* 2001;124:1396–402
15. Sailer M, Losseff NA, Wang L, et al. **T1 lesion load and cerebral atrophy as a marker for clinical progression in patients with multiple sclerosis: a prospective 18 months follow-up study.** *Eur J Neurol* 2001;8:37–42
16. Barkhof F. **The clinico-radiological paradox in multiple sclerosis revisited.** *Curr Opin Neurol* 2002;15:239–45
17. Barkhof F, Karas GB, van Walderveen MA. **T1 hypointensities and axonal loss.** *Neuroimaging Clin N Am* 2000;10:739–52
18. van Walderveen MA, Barkhof F, Hommes OR, et al. **Correlating MRI and clinical disease activity in multiple sclerosis: relevance of hypointense lesions on short-TR/short-TE (T1-weighted) spin-echo images.** *Neurology* 1995;45:1684–90
19. van Walderveen MA, Kamphorst W, Scheltens P, et al. **Histopathologic correlate of hypointense lesions on T1-weighted spin-echo MRI in multiple sclerosis.** *Neurology* 1998;50:1282–88
20. Bitsch A, Kuhlmann T, Stadelmann C, et al. **A longitudinal MRI study of histopathologically defined hypointense multiple sclerosis lesions.** *Ann Neurol* 2001;49:793–96
21. Barkhof F, Bruck W, De Groot CJ, et al. **Remyelinated lesions in multiple sclerosis. Magnetic resonance imaging appearance.** *Arch Neurol* 2003;60:1073–81
22. Bruck W, Bitsch A, Kolenda H, et al. **Inflammatory central nervous system demyelination: correlation of magnetic resonance imaging findings with lesion pathology.** *Ann Neurol* 1997;42:783–93
23. Lassmann H. **The pathological substrate of magnetic resonance alterations in multiple sclerosis.** *Neuroimag Clin N Am* 2008;18:563–76
24. Ikonomidou VN, van Gelderen P, de Zwart JA, et al. **Optimizing brain tissue contrast with EPI: a simulated annealing approach.** *Magn Res Med* 2005;54:373–85
25. Bottomley PA, Foster TH, Argensinger RE, et al. **A review of normal tissue hydrogen NMR relaxation times and relaxation mechanisms from 1–100 MHZ: dependence on tissue type, NMR frequency, temperature, species, excision and age.** *Med Phys* 1984;11:425–48
26. Poser CM, Paty DW, Scheinberg L, et al. **New diagnostic criteria for multiple sclerosis: guidelines for research protocols.** *Ann Neurol* 1983;13:227–31
27. Kurtzke JF. **Rating neurologic impairment in multiple sclerosis: an expanded disability status scale (EDSS).** *Neurology* 1983;33:1444–52
28. Fischer JS, Rudick RA, Cutter GR, et al. **The Multiple Sclerosis Functional Composite Measure (MSFC): an integrated approach to MS clinical outcome assessment. National MS Society Clinical Outcomes Assessment Task Force.** *Mult Scler* 1999;5:244–50
29. Richert ND, Ostuni JL, Bash CN, et al. **Interferon beta-1b and intravenous methylprednisolone promote lesion recovery in multiple sclerosis.** *Mult Scler* 2001;7:49–59
30. Cohen MS, DuBois RM, Zeineh MM. **Rapid and effective correction of RF inhomogeneity for high field magnetic resonance imaging.** *Hum Brain Mapp* 2000;10:204–11
31. Filippi M, Gawne-Cain ML, Gasperini C, et al. **Effect of training and different measurement strategies on the reproducibility of brain MRI lesion load measurements in multiple sclerosis.** *Neurology* 1998;50:238–44
32. Richert ND, Ostuni JL, Bash CN, et al. **Serial whole-brain magnetization transfer imaging in patients with relapsing-remitting multiple sclerosis at baseline and during treatment with interferon beta-1b.** *AJNR Am J Neuroradiol* 1998;19:1705–13
33. Smith SM, Zhang Y, Jenkinson M, et al. **Accurate, robust, and automated longitudinal and cross-sectional brain change analysis.** *Neuroimage* 2002;17:479–89
34. Bagnato F, Butman JA, Mora CA, et al. **Conventional magnetic resonance imaging features in patients with tropical spastic paraparesis.** *J Neurovirol* 2005;11:525–34
35. Redpath TW, Smith FW. **Technical note: use of a double inversion recovery pulse sequence to image selectively grey or white brain matter.** *Br J Radiol* 1994;67:1258–63
36. Wattjes MP, Lutterbey GG, Gieseke J, et al. **Double inversion recovery brain imaging at 3T: diagnostic value in the detection of multiple sclerosis lesions.** *AJNR Am J Neuroradiol* 2007;28:54–59
37. Moraal B, Roosendaal SD, Pouwels PJ, et al. **Multi-contrast, isotropic, single-slab 3D MR imaging in multiple sclerosis.** *Eur Radiol* 2008;18:2311–20
38. Madelin G, Oesingmann N, Inglese M. **Double inversion recovery MRI with fat suppression at 7 Tesla: initial experience.** *J Neuroimaging* 2008 Nov 6. [Epub ahead of print]
39. van Waesberghe JHTM, Kamphorst W, De Groot CJA, et al. **Axonal loss in multiple sclerosis lesions: magnetic resonance imaging insights into substrates of disability.** *Ann Neurol* 1999;46:747–54
40. Schmierer K, Scaravilli F, Altmann DR, et al. **Magnetization transfer ratio and myelin in postmortem multiple sclerosis brain.** *Ann Neurol* 2004;56:407–15
41. Giugni E, Pozzilli C, Bastianello S, et al. **MRI measures and their relations with clinical disability in relapsing-remitting and secondary progressive multiple sclerosis.** *Mult Scler* 1997;3:221–25
42. Zivadinov R, Stosic M, Cox JL, et al. **The place of conventional MRI and newly emerging MRI techniques in monitoring different aspects of treatment outcome.** *J Neurol* 2008;255:61–74
43. Bermel RA, Bakshi R. **The measurement and clinical relevance of brain atrophy in multiple sclerosis.** *Lancet Neurol* 2006;5:158–70